



**HAL**  
open science

# Extreme tropical cyclone activities in the southern Pacific Ocean

Karl Hoarau, Ludovic Chalonge, Florence Pirard, Daniel Peyrusaubes

► **To cite this version:**

Karl Hoarau, Ludovic Chalonge, Florence Pirard, Daniel Peyrusaubes. Extreme tropical cyclone activities in the southern Pacific Ocean. *International Journal of Climatology*, 2018, 38 (3), pp.1409-1420. 10.1002/joc.5254 . hal-04431570

**HAL Id: hal-04431570**

**<https://univ-montpellier3-paul-valery.hal.science/hal-04431570>**

Submitted on 1 Feb 2024

**HAL** is a multi-disciplinary open access archive for the deposit and dissemination of scientific research documents, whether they are published or not. The documents may come from teaching and research institutions in France or abroad, or from public or private research centers.

L'archive ouverte pluridisciplinaire **HAL**, est destinée au dépôt et à la diffusion de documents scientifiques de niveau recherche, publiés ou non, émanant des établissements d'enseignement et de recherche français ou étrangers, des laboratoires publics ou privés.

## Extreme tropical cyclone activities in the southern Pacific Ocean

Journal:	<i>International Journal of Climatology</i>
Manuscript ID	Draft
Wiley - Manuscript type:	Research Article
Date Submitted by the Author:	n/a
Complete List of Authors:	HOARAU, Karl; Cergy University, geography Chalonge, Ludovic; University of Paris 1 Pantheon - Sorbonne, geography PIRARD, Florence; Cergy University, Institute of Technology Peyrusaubes, Daniel; University of Poitiers, geography
Keywords:	southern Pacific Ocean, categories 4 and 5 cyclones, global warming, decadal variations, El Niño event

SCHOLARONE™  
Manuscripts

Only

1 **Extreme tropical cyclone activities in the southern Pacific Ocean**  
2  
3

4  
5 Karl HOARAU

6 University of Cergy-Pontoise, 33 Boulevard du Port

7 95011 Cergy Cedex, FRANCE, phone 01 34 25 64 34, fax 01 34 25 64 42

8 KHoarau@aol.com

9  
10  
11 Ludovic CHALONGE

12 University of Paris 1 Pantheon - Sorbonne, 13 rue du Four

13 75006 Paris, FRANCE

14  
15  
16 Florence PIRARD

17 University of Cergy-Pontoise, Institute of Technology, 95-97 rue Valere Collas

18 95100 Argenteuil, FRANCE

19  
20  
21 Daniel PEYRUSAUBES

22 University of Poitiers, 5 rue Theodore Lefebvre

23 86073 Poitiers, FRANCE  
24  
25  
26  
27  
28  
29  
30

31 **ABSTRACT:** This research concerning the South Pacific Ocean shows the ten-year and  
32 interannual variability of extreme cyclones (categories 4 and 5). The intensity of these  
33 cyclones has been reanalysed on the basis of GMS, GOES, and NOAA satellite images. In the  
34 period 1980 to 2016, 63 cyclones reached categories 4 and 5. During the decade 1980-89, the  
35 intensity of cyclones of at least 115 knots was underestimated: we found 19 such cyclones, as  
36 opposed to 6 in the Joint Typhoon Warning Center (JTWC) database. Between 1980 and  
37 2016, the number of extreme cyclones did not show any tendency to increase. The 1983  
38 season was the most active, with 6 cyclones of categories 4 and 5 that do not figure in the  
39 JTWC database for the South Pacific. El Niño episodes concurred with a much higher number  
40 of cyclones of at least 115 knots than La Niña episodes. More than half of the category 5 (at  
41 least 140 knots) cyclones were observed during El Niño years. While the ocean temperature is  
42 not a negligible explanatory factor, tropospheric dynamics remain determinant. The South  
43 Pacific Ocean is the theatre of very intense cyclones, comparable to those in the western or  
44 eastern North Pacific. Thus, by reanalysing satellite images, an intensity of 170 knots was  
45 attributed to cyclone Hina (March 1985), which was the strongest in the southern hemisphere  
46 since 1980.

47 **Key words:** southern Pacific Ocean; categories 4 and 5 cyclones; global warming; decadal  
48 variations; El Niño event.

49

50

51

52

53

54

## 55 1. Introduction

56 The South Pacific Ocean corresponds to the ocean basin located south of the equator and  
57 delimited in the west by the 135° East meridian. On average, every year, 10 tropical  
58 disturbances reach at least the tropical storm stage with 35 knots winds sustained for 1 minute  
59 (Diamond *et al.*, 2012; Walsh *et al.*, 2015). The present Joint Typhoon Warning Center's  
60 database (JTWC, 2015) shows that, on average, every year in the South Pacific Ocean, 1  
61 tropical storm increased in intensity to a category 4 or 5 extreme cyclone (at least 115 knots)  
62 in the Saffir-Simpson classification (Simpson, 1974). In the debate on global warming and the  
63 variation in the number of category 4 and 5 extreme cyclones, research has produced very  
64 different results for the South Pacific Ocean. Webster *et al.* (2005) found that activity doubled  
65 between 1975-1989 and 1990-2004. Klotzbach (1986) indicates a moderate trend (+23%)  
66 towards an increase in the number of cyclones of at least 115 knots between 1986-1995 and  
67 1996-2005 in the South Pacific. Kuleshov *et al.* (2010) have not mentioned any trend for the  
68 period 1982 to 2007. More recently, Klotzbach and Landsea (2015) have not revealed any  
69 trend between 1990 and 2014. These various research studies used existing archives  
70 concerning the intensity of cyclones of which the data had never been verified. On the basis of  
71 an automatic algorithm applied to satellite images, Kossin *et al.* (2007) estimated the intensity  
72 of cyclones on the worldwide scale between 1983 and 2005. Apart from the fact that this  
73 method reduces the accuracy of the estimated intensity compared to the Dvorak classic  
74 method (1984), Kossin *et al.* (2007) did not find any trend in the number of categories 4 and 5  
75 cyclones for the South Pacific. In order to provide new light, this article deals with the  
76 original elements of the activity of category 4 and 5 extreme tropical cyclones in the South  
77 Pacific, based on the reanalysis of satellite images during the period 1980-2016.

## 78 2. Under-estimation of the intensity of cyclones in the decade 1980-1989.

79 The South Pacific Ocean was served for the period 1980-2016 by two geostationary satellites,  
80 GMS positioned at 140°E, and GOES-West at 135°W (Foley, 1995). While GMS satellites  
81 have always had a resolution of 4 km with infrared, GOES satellites had 8 km resolution in  
82 the 1980s. Also, these satellites could not always observe the real temperature of the warmest  
83 pixel in the eye of cyclones, considering the position of the cyclones or the small size of the  
84 eye. The temperature of the eye is an important parameter for estimating the intensity of  
85 cyclones from infrared images. Consequently, it was necessary to use images with 4 km  
86 resolution from polar orbiting satellites belonging to the National Oceanic and Atmospheric  
87 Administration (NOAA). While moving, these satellites can pass directly above cyclones and  
88 observe the warmest pixel in the eye. Indeed, the stage of intensity of a cyclone is determined  
89 by the Dvorak (1984) analysis, for which one needs to know the highest temperature in the  
90 eye and the temperature of the top of the clouds within a radius of 0.5 degree around the  
91 cyclone centre. The Dvorak Technique is based on cyclone operational procedures that are  
92 used to estimate the intensity by means of the maximum sustained wind over 1 minute. This  
93 Technique was published in 1984. Since forecasters need several months to learn about and  
94 experience this technique, an efficient application was effective in all the world's cyclone  
95 basins in the late 1980s (Knaff *et al.*, 2010). Furthermore, the assessment of the Dvorak  
96 Technique did not find any overestimation of the intensity of the strongest cyclones.

97 To illustrate the problem of the insufficient quality of databases concerning the intensity of  
98 cyclones pointed out by several authors (Landsea *et al.*, 2006; Harper *et al.*, 2008; Hoarau *et*  
99 *al.*, 2012) including Kuleshov *et al.* (2010) on the subject of the South Pacific Ocean, we took  
100 the example of Isaac (22P), whose intensity is not known in the JTWC database (2015). This  
101 cyclone formed on 28 February 1982 east of the Samoa Islands and then moved towards the  
102 south-west (Figure 1).

103

104

**Figure 1**

105

106 On examining satellite images, marked cooling of the cloud tops was noted between the start  
107 and the middle of the day on 1 March (Figure 2), when Isaac's cloud configuration  
108 corresponded to 4.5 on the Dvorak (1984) scale, which goes up to 8.

109

**Figure 2**

110 The intensity is therefore estimated at 75 knots (Figure 3). On 2 March, the increase in  
111 intensity continues rapidly.

112

**Figure 3**

113 At 0600 UTC, a small eye forms in the central dense overcast (Figure 2). The eye widens and  
114 warms up to +18.4°C at 1500 UTC. The wide cloud belt of 0.5 degree includes tops with  
115 temperatures of -70°C to -77°C. The more the eye is warm and the more the cloud tops are  
116 cold, the greater is the intensity of the cyclone. At 1200 UTC and 1500 UTC, Isaac displayed  
117 satellite data of 7.0, which, in the Dvorak Technique, match with sustained winds of 140  
118 knots. However, at 1800 UTC, satellite data figures drop to 6. This is why the maximum  
119 intensity of the cyclone is estimated at 130 knots (category 4) at 1500 UTC and 1800 UTC  
120 before its intensity starts decreasing (Figure 3). During a phase of rapid intensification, winds  
121 do not have time to adjust to the cloud configuration, and the same applies during a phase of  
122 rapid decrease (on 3 March from 0600 UTC): an increase or decrease of the strength of winds  
123 in the cyclone is delayed by a few hours in relation to satellite data.

124

125 Cyclone Isaac is not an isolated case. Comparison of our reanalysis with the JTWC database  
126 (2015) shows that the number of category 4 and 5 cyclones had been largely underestimated  
127 in the South Pacific during the decade 1980-89 (Figure 4): we found 19 cyclones that  
128 generated winds of at least 115 knots, as opposed to 6 found by JTWC. The ten-year  
distribution between 1980 and 2009 does not show a trend towards an increase in the number

129 of category 4 and 5 cyclones, even if activity in the present decade 2010-19 should be higher  
130 than activity in 2000-09.

131 **Figure 4**

132 When one considers the location of the maximum intensity of each of the 63 extreme cyclones  
133 in the South Pacific from 1980 to 2016, one finds that the geographical area concerned ranges  
134 from 10°S to 23°S and from 135°E to 145°W (figure 5). A total of 44 (70%) of the 63  
135 category 4 and 5 cyclones, and 12 (66%) of the 18 category 5 cyclones (at least 140 knots)  
136 reached their maximum intensity west of the 180° meridian.

137 **Figure 5**

138 In the 1980s, a category 5 cyclone was observed at 147°W. It is the most intense cyclone  
139 listed in the south-eastern part of the Pacific Ocean. Most of the extreme cyclones reached  
140 their maximum between 12°S and 18°S. The four category 4 cyclones (115 to 135 knots) that  
141 reached their maximum intensity south of 20°S have occurred since 2010. This could confirm  
142 the poleward migration of the location of the maximum intensity of cyclones identified by  
143 Kossin *et al.* (2014). These different characteristics of the extreme cyclones activity in the  
144 South Pacific are greatly influenced by the interannual variations of oceanic and tropospheric  
145 conditions.

### 146 **3. The indisputable role of the El Niño phenomenon**

147 Marked interannual variability of the number of category 4 and 5 cyclones was found in the  
148 South Pacific (Figure 6). The maximum was 6 extreme cyclones during the summer of 1983,  
149 while none was observed 7 times between 1980 and 2016.

150 **Figure 6**

151 The 1983 season was under the influence of a strong El Niño episode (CPCM, 2016). None of  
152 the 6 extreme cyclones in 1983 is found in the JTWC database (2014) with an intensity of



153 more than 100 knots (Figure 7), while our reanalysis finds sustained winds over 1 minute  
154 ranging from 120 knots in the case of Tomasi (19P) on 30 March to 155 knots (7.5 on the  
155 Dvorak's scale) for Orama (13P) on 24 February.

156 **Figure 7**

157 Orama is the strongest cyclone in the eastern part of the basin. In the same year, Reva (17P)  
158 and Veena (21P) respectively reached 125 and 130 knots east of the 150°W meridian. While  
159 the two other strong El Niño episodes, in 1998 and 2016, did not concur with a high number  
160 of extreme cyclones (of which there were 2 in each of these years), the most moderate El  
161 Niños in 1992, 2003 and 2005 had more activity (Figure 6). In total, during the 9 El Niño  
162 episodes from 1980 to 2016, there were 28 category 4 and 5 cyclones, i.e., an average of 3.1  
163 per year. This is a higher value than the average of 1.7 per year, if we count the 63 cyclones  
164 that occurred in 37 years. However, the 8 La Niña episodes produced 10 extreme cyclones,  
165 with an annual average of 1.25, a value comparable to that obtained on the basis of 25  
166 extreme cyclones formed during the 20 other seasons in the South Pacific. Therefore,  
167 cyclones were of greater intensity during El Niño phases, and their location at the time of their  
168 maximum intensity was different from that of La Niña episodes or other seasons (Figure 8).

169 **Figure 8**

170 Among the 18 category 5 cyclones (at least 140 knots), 10 (55.55%) were observed during the  
171 9 El Niño episodes, 3 (16.66%) during the 8 La Niña phases, and 5 (27.79%) during the 20  
172 other seasons. During the El Niño episodes, category 4 and 5 cyclones reached their  
173 maximum between 160°E and 147°W, with a centre of gravity located around 15.5°S and  
174 173°W. During La Niña phases, extreme cyclones reached their maximum at a position  
175 further west and further south, with a centre of gravity around 17.5°S and 160°E; no cyclone  
176 reached category 4 or 5 east of the 180° meridian. For the 20 other seasons, the centre of  
177 gravity was located at 16.5°S and 163°E. Concerning the differences of location between El

178 Niño and La Niña, our results for extreme cyclones concur with those found by several  
179 authors who worked on the tropical storms and cyclones of the hurricane stage in the South  
180 Pacific Ocean (Nicholls, 1979, 1984; Revel and Gouter, 1986; Basher and Zheng, 1995;  
181 Chand and Walsh, 2011; Dowdy *et al.*, 2012; Chand *et al.*, 2013).

182 In addition, we compared the temperature of the ocean, firstly, between the 2 strongest El  
183 Niño episodes, and secondly, between the 2 most marked La Niña phases (CPCM, 2016).

184 While the ocean temperature was higher in the South Pacific for El Niño in the summer of  
185 2016 than in 1983 (Figure 9), the number of extreme cyclones was higher, and activity  
186 extended further to the east in 1983.

187 **Figure 9**

188 Similarly, the ocean temperature was higher for La Niña in the summer of 2000 than in 1989  
189 (Figure 10), and there were no extreme cyclones in 2000, as opposed to 2 in 1989. Therefore,  
190 it is not only the higher ocean temperature in the eastern South Pacific during an El Niño  
191 phase that explains the higher number of cyclones of at least 115 knots east of the 180°  
192 meridian.

193 **Figure 10**

194 At the same time, the absence of category 4 and 5 cyclones east of the 180° meridian during  
195 the La Niña episodes cannot be explained by the ocean temperature, which was at least 28°C  
196 in February 1989 and 2000. Consequently, the conditions in the troposphere are determinant  
197 in the South Pacific Ocean. During the El Niño, the cyclonic vorticity of low layers is stronger  
198 in the monsoon trough that occupies a position between 170 degrees East and 140 degrees  
199 West (Dowdy *et al.*, 2012; Chand *et al.*, 2013). Vertical wind shear reaches low figures to the  
200 east of the 180° meridian, with winds at 200 hPa which have an eastward component (Basher  
201 and Zheng, 1995; Ramsay *et al.*, 2008; Dowdy *et al.*, 2012; Chand *et al.*, 2013; Cheung *et al.*,  
202 2014). Thus the eastward extension of favourable atmospheric conditions enables tropical

203 storms to develop and to become category 4 and 5 cyclones. During La Niña phases, the  
204 formation and intensification of cyclones take place in the western part of the ocean basin  
205 with unfavourable atmospheric conditions east of the 180° meridian.

#### 206 **4. The strongest cyclones in the South Pacific Ocean**

207 It is always difficult to determine what are the most intense cyclones in a specific basin. Nott  
208 *et al.* (2014) put forward a pressure of 880 hPa for cyclone Mahina on the basis of the  
209 9 metres storm tide that had hit Bathurst Bay in North-East Australia and a measurement of  
210 914 hPa observed by a boat on 5 March 1899. Even if the authors consider Mahina to be the  
211 most intense cyclone ever recorded in the southern hemisphere, it is not possible to attribute  
212 an intensity to a cyclone for which there is no satellite data or wind data. In the JTWC  
213 database (2015), 2 cyclones were estimated at 155 knots in the South Pacific, that is, Zoe  
214 (06P) on 27 December 2002, and Monica (23P) on 23 April 2006. In real time, JTWC  
215 attributed an intensity of 155 knots to cyclone Winston (11P) on 20 February 2016. In a  
216 detailed study, Durden (2010) estimated Monica at 160 knots. Our reanalysis of satellite  
217 images of the South Pacific between 1980 and 2016 also enabled us to list the strongest  
218 cyclones. We identified cyclones that reached sustained winds of at least 155 knots, i.e., 7.5  
219 on the Dvorak (1984) scale. In the satellite imagery, these cyclones are seen to have an eye  
220 with a temperature of more than +9°C, and with cloud tops colder than -75°C within a  
221 minimum radius of 0.5 degree around the centre. This was the case for Orama (Figure 7) and  
222 for the 3 cyclones already mentioned – Zoe, Monica and Winston – to which we added  
223 cyclones Anne (07P) on 10 January 1988 and Percy (20P) on 2 March 2005 (Figure 11),  
224 which have an intensity of 140 knots in the JTWC database (2015). During its phase of very  
225 rapid intensification, satellite data showed that Anne even reached 8 on the Dvorak (1984)  
226 scale, with clouds top temperature between -81°C and -90°C (Figure 11). However, this cloud

227 configuration did not remain long enough to allow this cyclone to be estimated at more than  
228 155 knots.

229 **Figure 11**

230 In agreement with Durden (2010), our analysis attributes 160 knots to Monica. In fact, a  
231 seventh cyclone exceeded 155 knots and, below, we study it in more detail, because it may be  
232 considered as the most intense cyclone in the South Pacific.

233 This is cyclone Hina (30P), which was formed on 13 and 14 March 1985 north of the Vanuatu  
234 Islands (Figure 12). This cyclone moved at more than 15 knots in the east-south-east  
235 direction, then south-east, passing to the west of the Fiji Islands at the end of the day on 16  
236 March.

237 **Figure 12**

238 From its very beginning, Hina intensified rapidly, increasing from 55 knots to 105 knots in 24  
239 hours between 14 and 15 March at 0000 UTC (Figure 13). It is at that time that our analysis  
240 starts to diverge from that of JTWC, which attributed a maximum intensity of 135 knots to  
241 Hina on 16 March at 0600 UTC and 1200 UTC. For the same period, our estimation gives 170  
242 knots, i.e., an intensity of 8 on the Dvorak (1984) scale.

243 **Figure 13**

244 Cyclone Hina had a cloud configuration of 140 knots on 15 March at 0300 UTC, 155 knots at  
245 0600 UTC, and 170 knots on 16 January from 0300 UTC to 1200 UTC. The persistence of  
246 satellite data at 155-170 knots for a period of more than 24 hours enabled sustained winds to  
247 gradually adjust to the cloud scheme, explaining the exceptional intensity reached by cyclone  
248 Hina. The satellite imagery shows that Hina had cold cloud tops from the beginning of the day  
249 on 15 March (Figure 14). These cloud tops continued to cool while the eye was becoming  
250 warmer.

251 **Figure 14**

252

253 Thus the closed cloud belt that included cloud tops colder than  $-81^{\circ}\text{C}$  was extended to reach  
254 0.5 degree at its narrowest part on 16 January from 0300 UTC, 0.6 degree at 0600 UTC, and  
255 0.65 degree at 0900 UTC. At this time, certain cloud tops had a temperature of  $-92^{\circ}\text{C}$  just  
256 around the eye. The perfectly circular eye with a diameter of 22 km had a temperature of  
257  $+15^{\circ}\text{C}$  on 15 January at 0330 UTC,  $+18^{\circ}\text{C}$  at 1441 UTC,  $+21^{\circ}\text{C}$  on 16 January at 0319 UTC,  
258 and still  $+20^{\circ}\text{C}$  at 1500 UTC at the time when the cyclone started to weaken.

259 With an estimated intensity of 170 knots, Hina is probably the strongest cyclone in the  
260 southern hemisphere since the early 1980s. JTWC (2015) attributed winds of 150 knots to  
261 cyclone Agnielle (01S) on 21 November 1995 in the South Indian Ocean – an intensity  
262 similar to that attributed in real time to cyclone Fantala (19S) on 18 April 2016. However,  
263 there has still not been a reanalysis of cyclone intensities in this basin. Nevertheless, Hina  
264 could be one of the world's most intense cyclones since 1980. Only Patricia on 23 October  
265 2015 in the North-East Pacific and Haiyan on 7 November 2013 in the North-West Pacific  
266 reached respectively 185 knots (Kimberlain *et al.*, 2016) and 170 knots (Lander *et al.*, 2014).

## 267 **5. Conclusion**

268 This study highlighted the particularities of category 4–5 extreme tropical cyclones in the  
269 southern Pacific Ocean over the period 1980-2016. The re-analysis of intensities using  
270 satellite images indicates that 63 extreme cyclones were formed over the last 37 years. The  
271 number of category 4 and 5 cyclones had been largely underestimated in the South Pacific  
272 during the decade 1980-89; we found 19 cyclones that generated winds of at least 115 knots,  
273 as opposed to 6 found by JTWC. This illustrates the problem of the insufficient quality of  
274 databases and why a reanalysis of cyclone intensities was needed. The decadal distribution  
275 did not reveal any trend towards an increase in the number of these cyclones. In fact, the  
276 number of cyclones at least at 115 knots has decreased from 19 in the 1980s to 14 in the

277 2000s. However, since 2010, the extreme cyclone activity is going up and the four category 4  
278 cyclones (115 to 135 knots) that reached their maximum intensity south of 20°S have  
279 occurred since that year. 70% of the 63 category 4 and 5 cyclones and 66% of the 18 category  
280 5 cyclones (at least 140 knots) reached their maximum intensity west of the 180° meridian.

281 During the El Niño episodes, category 4 and 5 cyclones reached their maximum between  
282 160°E and 147°W, with a centre of gravity located around 15.5°S and 173°W. During La  
283 Niña phases, extreme cyclones reached their maximum at a position further west and further  
284 south, with a centre of gravity around 17.5°S and 160°E; no cyclone reached category 4 or 5  
285 east of the 180° meridian. For the 20 other seasons, the centre of gravity was located at 16.5°S  
286 and 163°E. Cyclones were of greater intensity during El Niño phases. The 9 El Niño episodes  
287 from 1980 to 2016 produced 28 category 4 and 5 cyclones, i.e., an average of 3.1 per year.  
288 The 8 La Niña episodes generated 10 extreme cyclones, with an annual average of 1.25, a  
289 value comparable to that obtained on the basis of 25 extreme cyclones formed during the 20  
290 other seasons in the South Pacific.

291 While the ocean temperature was higher in the South Pacific for El Niño than for La Niña,  
292 especially east of the 180° meridian, tropospheric dynamics remain determinant. During El  
293 Niño events, the eastward extension of favourable atmospheric conditions enables tropical  
294 storms to reach category 4 and 5 cyclones until 147°W. During La Niña phases, the  
295 intensification of cyclones takes place in the western part of the ocean basin with  
296 unfavourable atmospheric conditions east of the 180° meridian whereas the sea surface  
297 temperature was at least at 28°C.

298 Even if the southern Pacific Ocean is not the more active cyclonic basin, seven extreme  
299 cyclones have reached an intensity of at least 155 knots between 1980 and 2016. Orama, Hina  
300 and Anne formed in the 1980's; Zoe, Percy and Monica reached their peak in the 2000's. And  
301 Winston is the only cyclone at 155 knots for the period 2000-2016. Therefore, there is no

302 trend towards an increase of the strongest cyclones of the category 5. Moreover, our re-  
303 analysis shows that one cyclone, Hina in 1985, is estimated to have peaked at 170 knots. Hina  
304 is probably the more intense cyclone in the southern hemisphere since the early 1980s. Hina  
305 could be one of the world's most intense cyclones since the satellite era with typhoon Haiyan  
306 (November 2013) and hurricane Patricia (October 2015).

### 307 **Acknowledgements**

308 This work was funded by the University of Cergy-Pontoise, France. Grateful  
309 acknowledgements is made of the valuable comments by the reviewers.

### 310 **References**

- 311 Basher RE, Zheng X, 1995. Tropical cyclones in the southwest Pacific: Spatial patterns and  
312 relationships to Southern Oscillation and sea surface temperature. *Journal of Climate* **8**: 1249-  
313 1260.
- 314 Chand SS, Walsh KJE, 2011. Influence of ENSO on tropical cyclone intensity in the Fiji  
315 region. *Journal of Climate* **24**: 4096-4108.
- 316 Chand SS, McBride JL, Tory KJ, Wheeler MC, Walsh KJE, 2013. Impact of different ENSO  
317 regimes on southwest Pacific tropical cyclones. *Journal of Climate* **26**: 600-608.
- 318 Cheung KKW, Jiang N, Liu KS, Chan LTS, 2014. Interdecadal shift of intense tropical  
319 cyclone activity in the Southern Hemisphere. *International Journal of Climatology*, **34**, DOI:  
320 10.1002/joc.4073.
- 321 Climate Prediction Center Maryland (CPCM), 2016. The Oceanic Nino Index.  
322 [http://www.cpc.noaa.gov/products/analysis\\_monitoring/ensostuff/ensoyears.shtml](http://www.cpc.noaa.gov/products/analysis_monitoring/ensostuff/ensoyears.shtml)

- 323 Diamond HJ, Lorrey AM, Knapp KR, Levinson DH, 2012. Development of an enhanced  
324 tropical cyclone tracks database for the southwest Pacific from 1840 to 2010. *International*  
325 *Journal of Climatology* **32**: 2240-2250.
- 326 Dowdy AJ, Qi L, Jones D, 2012. Tropical Cyclone climatology of the South Pacific Ocean  
327 and Its Relationship to El Niño-Southern Oscillation. *Journal of Climate*, **25**: 6108-6122.
- 328 Durden SL, 2010. Remote Sensing and Modeling of Cyclone Monica near Peak Intensity.  
329 *Atmosphere*, **1**: 15-33.
- 330 Dvorak VF, 1984. Tropical cyclone intensity analysis using satellite data. *NOAA technical*  
331 *Report NESDIS 11*: 47p.
- 332 Foley GR, 1995. Observations and analysis of tropical cyclones. Global Perspectives on  
333 Tropical Cyclones. WMO/TD-No.693, Geneva: 1-20.
- 334 Harper BA, Stroud SA, McCormack M, West S, 2008. A review of historical tropical cyclone  
335 intensity in northwestern Australia and implications for climate change trend analysis.  
336 *Australian Meteorological Magazine*, **57**: 121-141.
- 337 Hoarau K, Bernard J, Chalonge L, 2012. Intense tropical cyclone activities in the northern  
338 Indian Ocean. *International Journal of Climatology*, **31**: 1935-1945.
- 339 Joint Typhoon Warning Center (JTWC), 2015. The tropical cyclones best track data in the  
340 southern hemisphere (1980-2015).  
341 [http://www.usno.navy.mil/NOOC/nmfc-ph/RSS/jtwc/best\\_tracks/shindex.php](http://www.usno.navy.mil/NOOC/nmfc-ph/RSS/jtwc/best_tracks/shindex.php)
- 342 Kimberlain TB, Blake ES, Cangialosi JP, 2016. Hurricane Patricia 20-24 October 2016  
343 (EP202015). *National Hurricane Center Tropical Cyclone Report*. NOAA, 32p.
- 344 Klotzbach PJ, 2006. Trends in global tropical cyclone activity over the past twenty years  
345 (1986-2005). *Geophysical Research Letters*, **33**, doi: 10.1029/2006GL025881.



- 346 Klotzbach PJ, Landsea CW, 2015. Extremely Intense Hurricanes: Revisiting Webster et al.  
347 (2005) after 10 Years. *Journal of Climate* **28**: 7621-7629.
- 348 Knaff JA, Brown DP, Courtney J, Gallina JG, Beven JL, 2010. An evaluation of Dvorak  
349 technique-based tropical cyclone intensity estimates. *Weather and Forecasting* **25**: 1362–  
350 1379.
- 351 Kossin JP, Knapp KR, Vimont DJ, Murnane RJ, Harper BA, 2007. A globally consistent  
352 reanalysis of hurricane variability and trends. *Geophysical Research Letters* **34**.  
353 10.1029/2006GL028836.
- 354 Kossin JP, Emanuel KA, Vecchi GA, 2014. The poleward migration of the location of  
355 tropical cyclone maximum intensity. *Nature*, **509**: 349-352.
- 356 Kuleshov Y, Fawcett R, Qi L, Trewin B, Jones D, McBride J, Ramsay H, 2010. Trends in  
357 tropical cyclones in the South Indian Ocean and the South Pacific Ocean. *Journal of*  
358 *Geophysical Research*, **115**, doi: 10.1029/2009JD012372.
- 359 Lander M, Guard C, Camargo SJ, 2014. State of the climate in 2013. *BAMS* **95**: 112-114.
- 360 Landsea CW, Harper BA, Hoarau K, Knaff JA, 2006. Can We Detect Trends in Extreme  
361 Tropical Cyclones? *Science*, **313**: 452-454.
- 362 Nicholls N, 1984. The Southern Oscillation, sea surface temperature, and interannual  
363 fluctuations in Australian tropical cyclone activity. *Journal of Climatology* **4**: 661-670.
- 364 Nicholls N, 1979. A possible method for predicting seasonal tropical cyclone activity in the  
365 Australian region. *Monthly Weather Review* **107**: 1221-1224.
- 366 Nott J, Green C, Townsend I, Callaghan J, 2014. The world record storm surge and the most  
367 intense southern hemisphere tropical cyclone, new evidence and modeling. *Bulletin of*  
368 *American Meteorological Society*, **95**: 757-765.

369 Ramsay HA, Leslie LM, Lamb PJ, Richman MB, Leplastrier M, 2008. Interannual Variability  
370 of Tropical Cyclones in the Australian Region: Role of Large-Scale Environment. *Journal of*  
371 *Climate* **21**: 1083-1103.

372 Revell CG, Goulter SW, 1986a. South Pacific tropical cyclones and the Southern Oscillation.  
373 *Monthly Weather Review* **114**: 1138-1145.

374 Simpson B, 1974. The Hurricane disaster potential scale. *Weatherwise*, **27**: 169-186.

375 Walsh KJE, McBride JL, Klotzbach PJ, Balachandran S, Camargo SJ, Holland G, Knutson  
376 TR, Kossin J, Lee TC, Sobel A, Sugi M, 2015. Tropical cyclones and climate change. *WIREs*  
377 *Clim Change* 2015. Doi: 10.1002/wcc.371.

378 Webster PJ, Holland GJ, Curry JA, Chang HR, 2005. Changes in tropical cyclone number,  
379 duration, and intensity in a warming environment. *Science*, **309**: 1844-1846.

#### 380 **Figure caption**

381 Figure 1. Trajectory of tropical cyclone Isaac (February-March 1982). Source: Chart created  
382 from data of JTWC.

383

384 Figure 2. Satellite images (Basic Dvorak) of cyclone Isaac. Source: Images treated using raw  
385 data from NCDC and JMA.

386

387 Figure 3. Estimation of the intensity of cyclone Isaac using the Dvorak method. Source: Chart  
388 created from raw data provided by GMS and NOAA.

389

390 Figure 4. Number of extreme category 4-5 cyclones per decade (1980-2016). Source: Chart  
391 prepared using data from JTWC and from the re-analysis of cyclone intensities by the authors.

392

393 Figure 5. The location of the maximum intensity of extreme cyclones in the southern Pacific  
394 Ocean. Source: Chart created from the re-analysis of cyclone intensities by the authors.

395

396 Figure 6. Annual number of extreme Cat 4-5 cyclones (1980-2016) and the El Niño, La Niña  
397 events. Source: Chart prepared using data from CPCM (2016) and the re-analysis of cyclone  
398 intensities by the authors.

399

400 Figure 7. Satellite images (Basic Dvorak) of extreme cyclones during the 1983 season.  
401 Source: Images treated using raw data from NCDC.

402

403 Figure 8. The location of the maximum intensity of extreme cyclones during El Niño, La Niña  
404 and the other seasons. Source: Chart prepared using data from CPMC (2016) and the re-  
405 analysis of cyclone intensities by the authors.

406

407 Figure 9. The location of the maximum intensity of extreme cyclones and the sea surface  
408 temperature during the two strongest El Niño events. Source: Chart prepared using data from  
409 NOAA/ESRL and from the re-analysis of cyclone intensities by the authors.

410

411 Figure 10. The location of the maximum intensity of extreme cyclones and the sea surface  
412 temperature during the two strongest La Niña events. Source: Chart prepared using data from  
413 NOAA/ESRL and from the re-analysis of cyclone intensities by the authors.

414

415 Figure 11. Satellite images (Basic Dvorak) of five of the seven strongest cyclones in the  
416 southern Pacific Ocean. Source: Images treated using raw data from NCDC.

417

418 Figure 12. Trajectory of tropical cyclone Hina (March 1985). Source: Chart created from data  
419 of JTWC.

420

421 Figure 13. Estimation of the intensity of cyclone Hina using the Dvorak method. Source:  
422 Chart created from raw data provided by GMS, NOAA and JTWC.

423

424 Figure 14. Satellite images (Basic Dvorak) of cyclone Hina. Source: Images treated using raw  
425 data from NCDC and JMA.

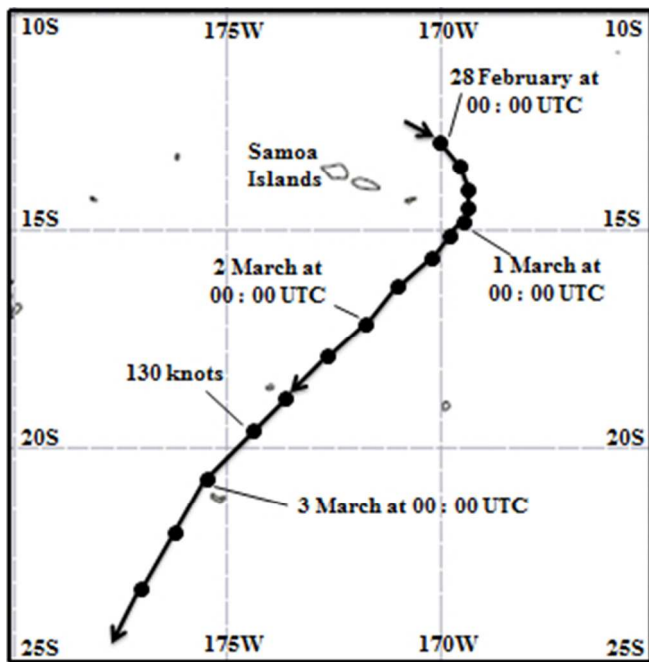


Figure 1. Trajectory of tropical cyclone Isaac (February-March 1982). Source: Chart created from data of JTWC.

114x116mm (72 x 72 DPI)

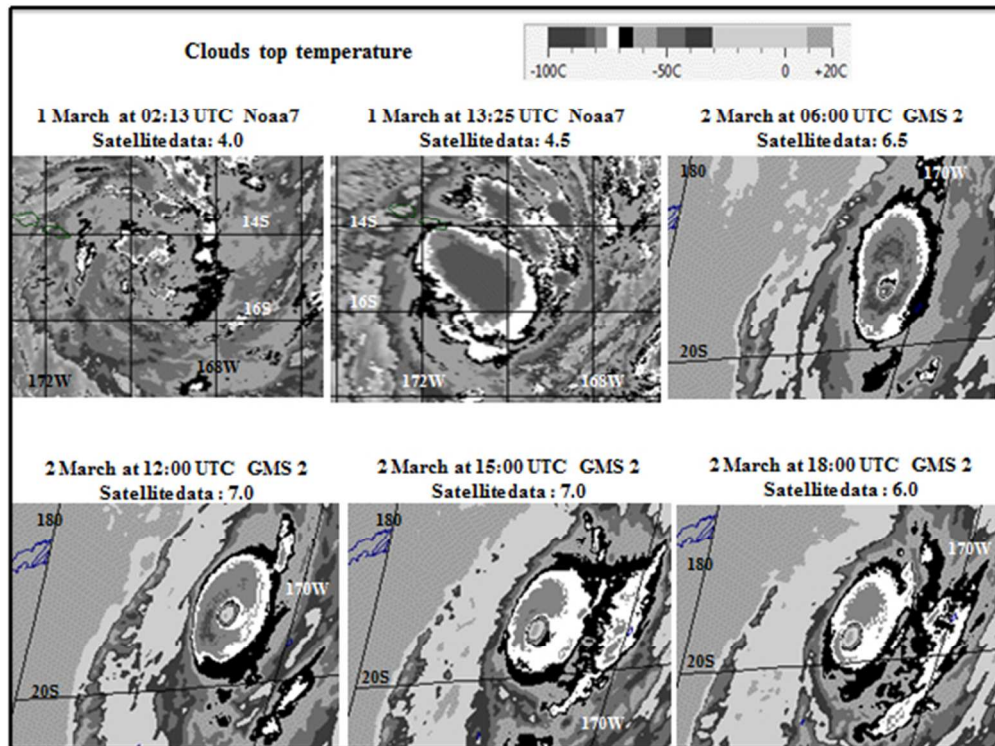


Figure 2. Satellite images (Basic Dvorak) of cyclone Isaac. Source: Images treated using raw data from NCDC and JMA.

203x152mm (72 x 72 DPI)

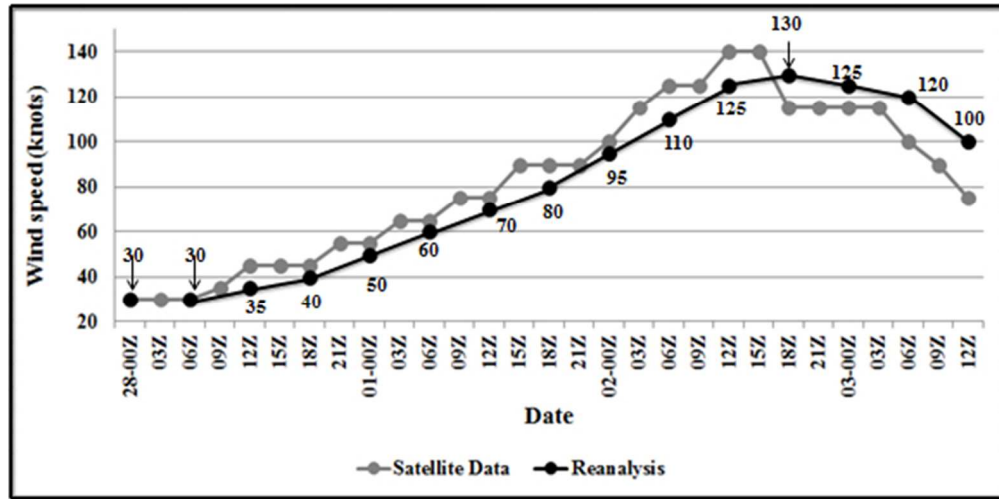


Figure 3. Estimation of the intensity of cyclone Isaac using the Dvorak method. Source: Chart created from raw data provided by GMS and NOAA.

204x101mm (72 x 72 DPI)

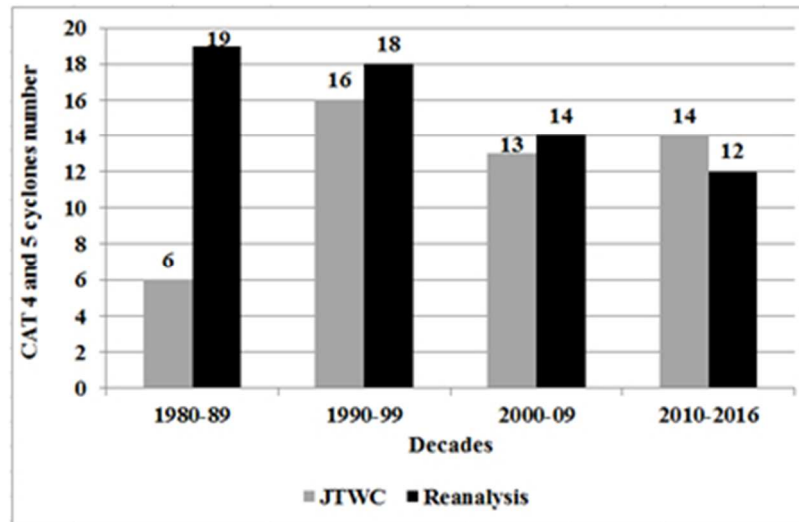


Figure 4. Number of extreme category 4-5 cyclones per decade (1980-2016). Source: Chart prepared using data from JTWC and from the re-analysis of cyclone intensities by the authors.

142x92mm (72 x 72 DPI)



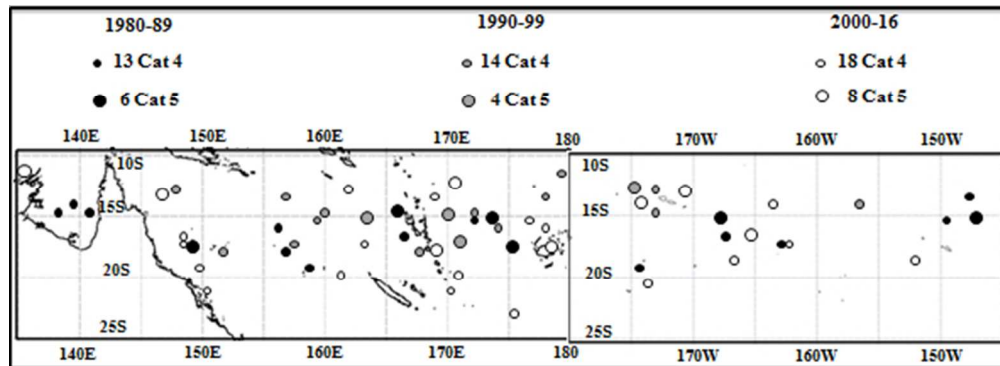


Figure 5. The location of the maximum intensity of extreme cyclones in the southern Pacific Ocean. Source: Chart created from the re-analysis of cyclone intensities by the authors.

208x76mm (72 x 72 DPI)

Review Only

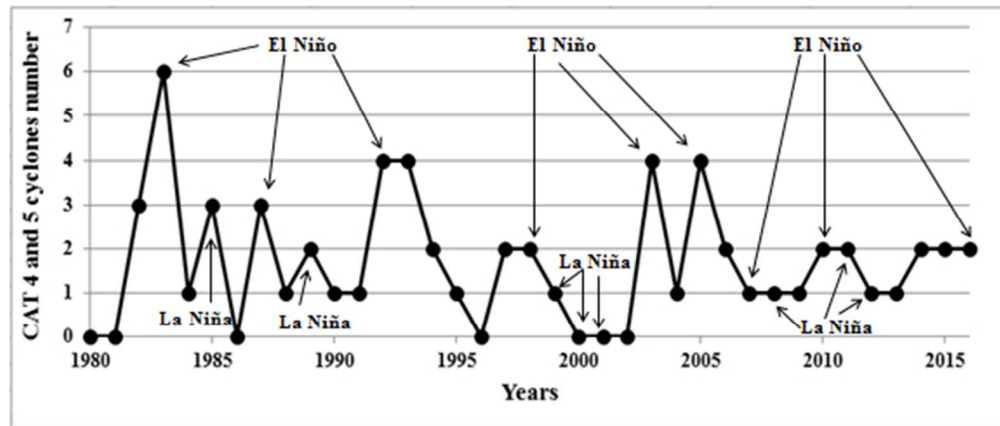


Figure 6. Annual number of extreme Cat 4-5 cyclones (1980-2016) and the El Niño, La Niña events. Source: Chart prepared using data from CPCM (2016) and the re-analysis of cyclone intensities by the authors.

203x86mm (72 x 72 DPI)

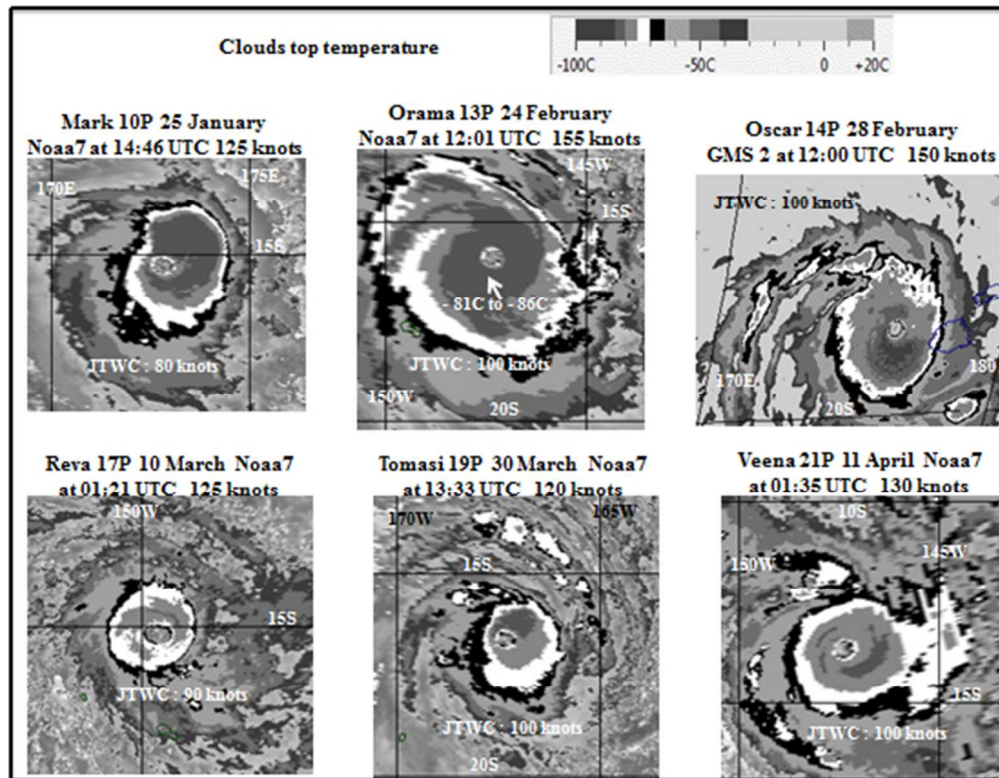


Figure 7. Satellite images (Basic Dvorak) of extreme cyclones during the 1983 season. Source: Images treated using raw data from NCDC.

194x150mm (72 x 72 DPI)

Only

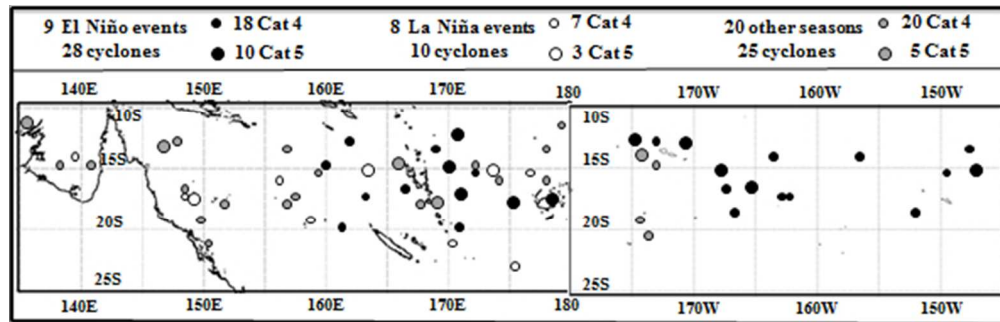


Figure 8. The location of the maximum intensity of extreme cyclones during El Niño, La Niña and the other seasons. Source: Chart prepared using data from CPMC (2016) and the re-analysis of cyclone intensities by the authors.

209x67mm (72 x 72 DPI)

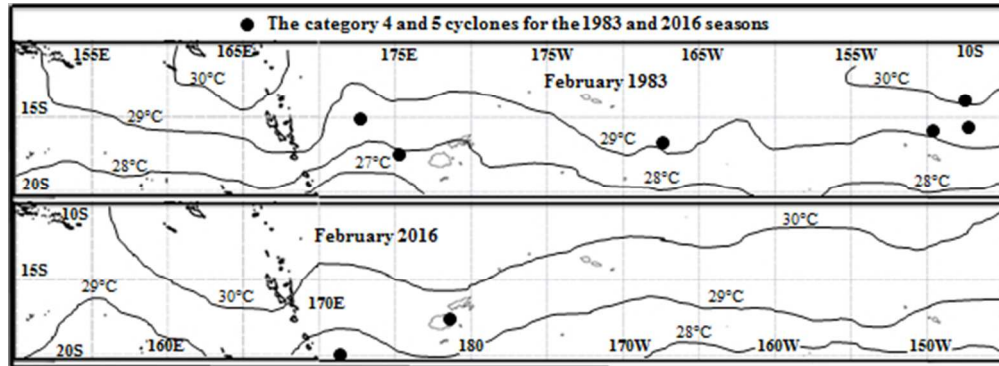


Figure 9. The location of the maximum intensity of extreme cyclones and the sea surface temperature during the two strongest El Niño events. Source: Chart prepared using data from NOAA/ESRL and from the re-analysis of cyclone intensities by the authors.

209x76mm (72 x 72 DPI)

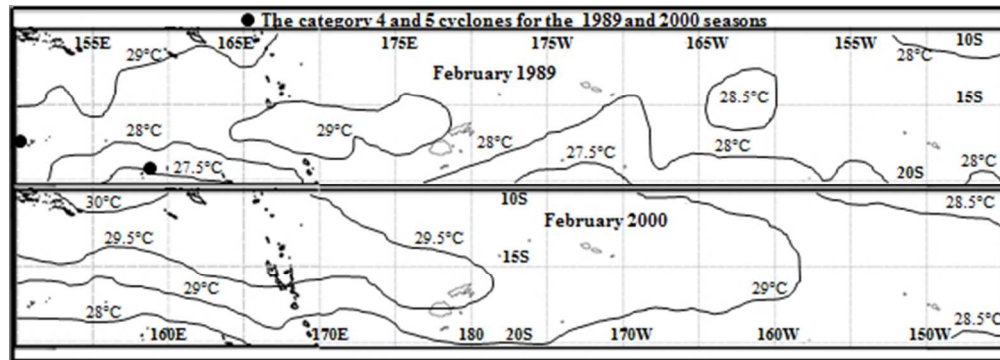


Figure 10. The location of the maximum intensity of extreme cyclones and the sea surface temperature during the two strongest La Niña events. Source: Chart prepared using data from NOAA/ESRL and from the re-analysis of cyclone intensities by the authors.

209x75mm (72 x 72 DPI)

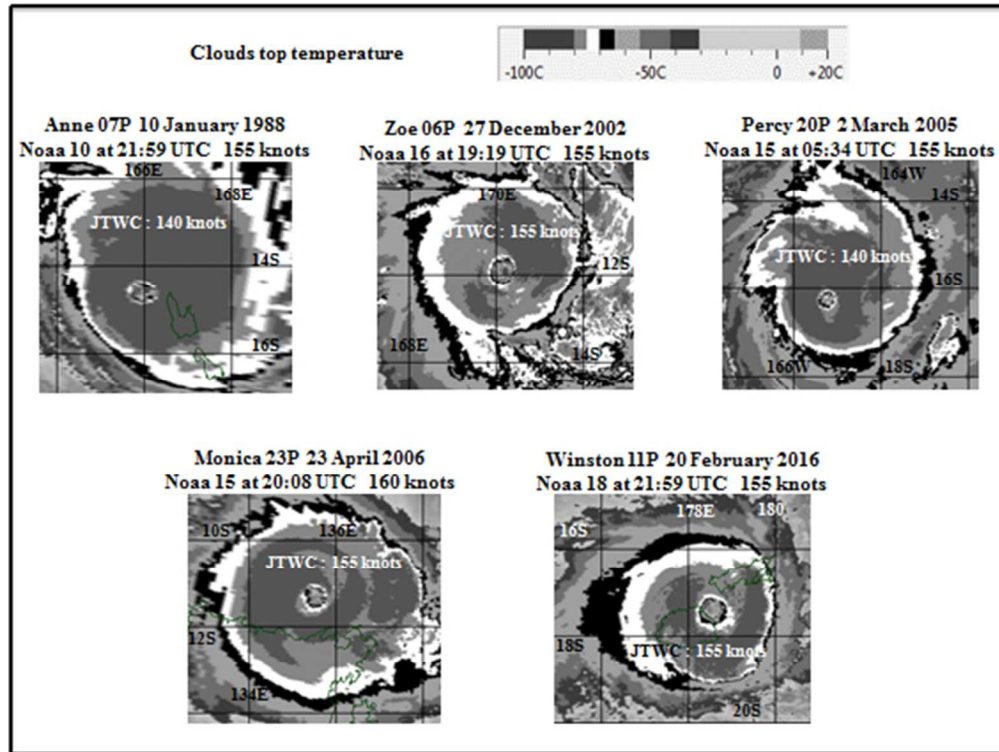


Figure 11. Satellite images (Basic Dvorak) of five of the seven strongest cyclones in the southern Pacific Ocean. Source: Images treated using raw data from NCDC.

199x150mm (72 x 72 DPI)

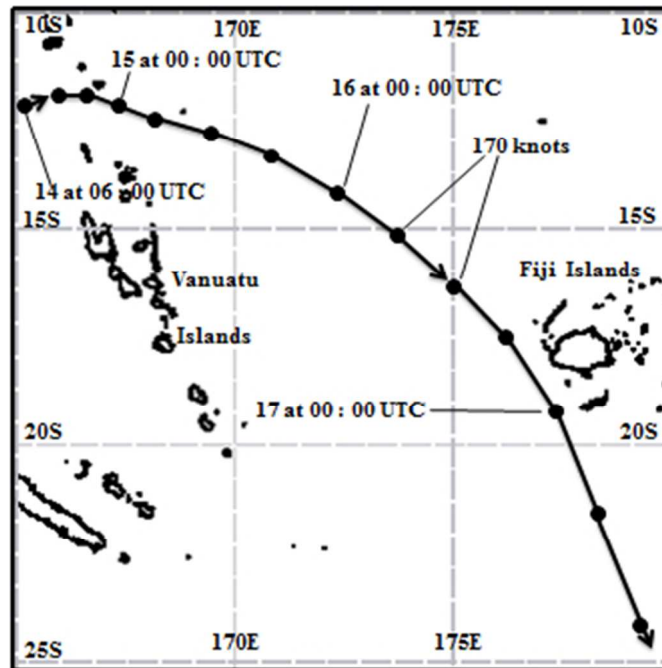


Figure 12. Trajectory of tropical cyclone Hina (March 1985). Source: Chart created from data of JTWC.

117x117mm (72 x 72 DPI)



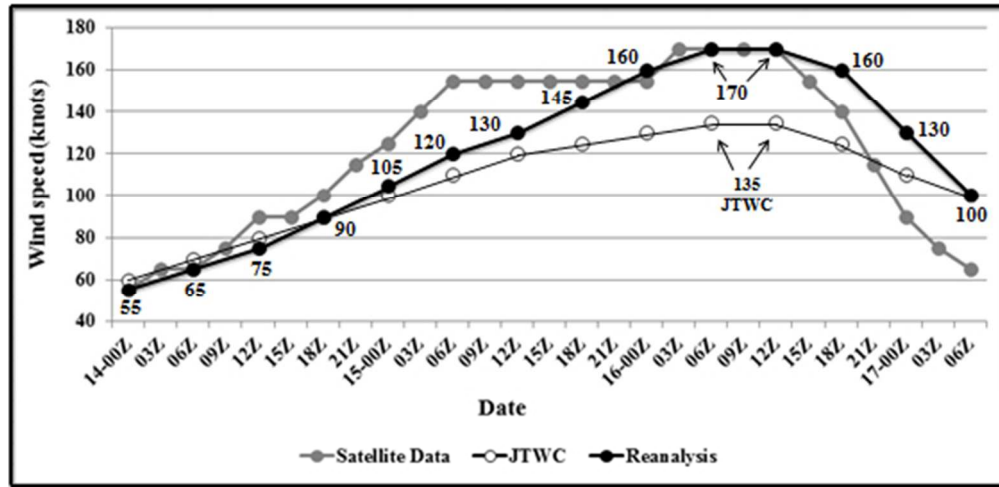


Figure 13. Estimation of the intensity of cyclone Hina using the Dvorak method. Source: Chart created from raw data provided by GMS, NOAA and JTWC.

197x95mm (72 x 72 DPI)

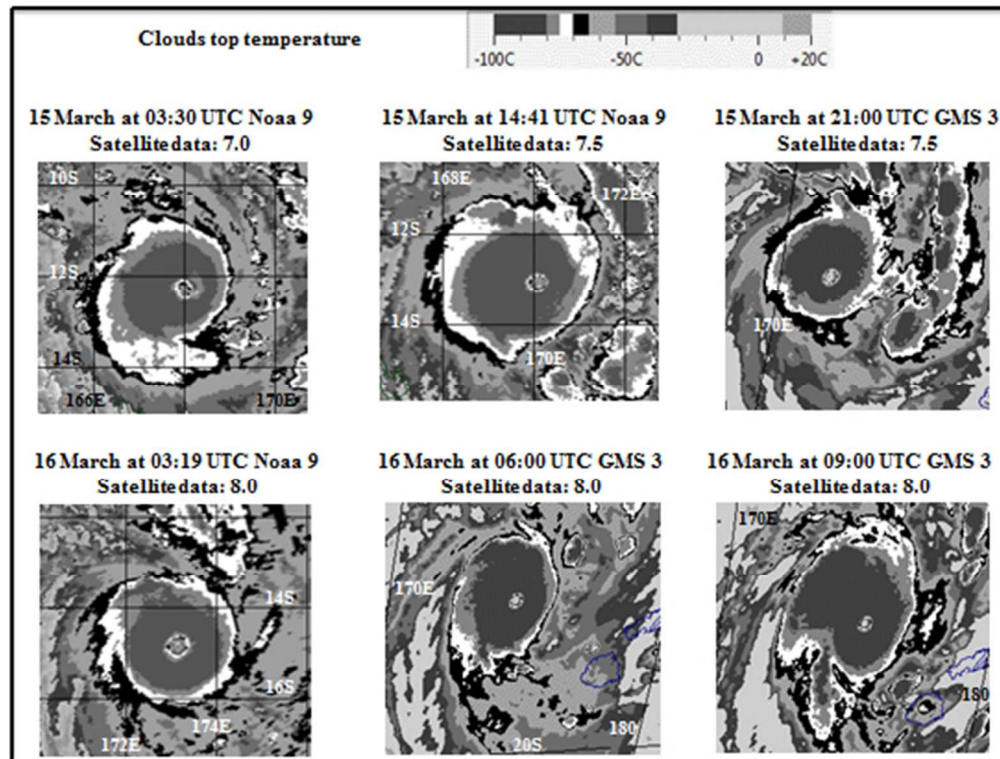


Figure 14. Satellite images (Basic Dvorak) of cyclone Hina. Source: Images treated using raw data from NCDC and JMA.

191x144mm (72 x 72 DPI)